IN VIVO EFFICACY OF ENGINEERED ACE2-FC IN PREVENTING LETHAL SARS-COV-2 INFECTION

D07

Yaozong Chen[1,8], Lulu Sun[2,8], Irfan Ullah[3,8], Guillaume Beaudoin-Bussières[4,5], Andrew P. Hederman[6], William D. Tolbert[1], Rebekah Sherburn[1], Dung N. Nguyen[1], Priti Kumar[6], Margaret E. Ackerman[6], Walther Mothes[7], Andrés Finzi[4,5], Pradeep D. Uchil[7], Frank J. Gonzalez[2], Marzena Pazgier[1#]

[1]Infectious Disease Division, Department of Medicine, Uniformed Services University of the Health Sciences, Bethesda, MD 20814-4712, USA. [2]Laboratory of Metabolism, Center for Cancer Research, National Cancer Institute, NIH, Bethesda, Maryland, USA. [3]Department of Internal Medicine, Section of Infectious Diseases, Yale University School of Medicine, New Haven, CT 06520, USA. [4]Centre de recherche du CHUM. Montreal, QC H2X 0A9, Canada. [5]Département de Microbiologie, Infectiologie et Immunologie, Université de Montréal, Montreal, QC H2X 0A9, Canada. [6]Thayer School of Engineering, Dartmouth College, Hanover, NH 03755, USA. [7]Department of Microbial Pathogenesis, Yale University School of Medicine, New Haven, CT 06510, USA. [8]equal contribution. [#]corresponding author (marzena.pazgier@usuhs.edu)

BACKGROUND

Soluble Angiotensin Converting Enzyme 2 (ACE2) constitutes an attractive therapeutic decoy with natural resistance to viral escape. To date, approaches using ACE2-Fc, a dimeric form of soluble ACE2, based on neutralizing activities, their potential as agents capable of Fc-effector functions, including antibody-dependent cellular cytotoxicity (ADCC), phagocytosis (ADCP) and complement deposition (ADCD) was largely unknown and has not been tested for effectiveness *in vitro*, or *in vivo*, in any model of SARS-CoV-2 infection.

METHODS

Structure-guided approaches was used to select the ACE2 mutations that improve SARS-CoV-2 spike (S) and knock-out angiotensin enzymatic activity. ACE2-Fcs variants were engineered in human IgG1 or IgG3 backbones and produced by mammalian HEK293 cell expression. The S binding was tested by ELISA and surface plasmon resonance (SPR). The mutations sites were validated by X-Ray crystallography. Neutralization activities were measured against SARS-CoV-2 variants of concern (VOCs) using *in vitro* pseudovirus (PsV) assay and dynamic bioluminescence imaging (BLI). ADCC and ADCP were tested using established methods. K18-hACE2 mice model infected by SARS-CoV-2 virus carrying nanoluciferase (nLuc) allows real-time bioluminenscence imaging (BLI) for viral spread in whole body and was used for prophylactic and therapeutic efficacy studies of engineered ACE2-Fcs with altered Fc-effector functions.

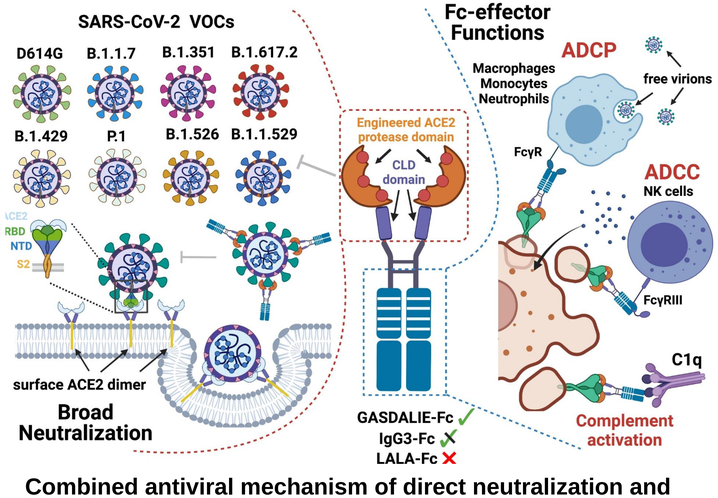

Combined antiviral mechanism of direct neutralization and Fc-effector functions by engineered ACE2-Fcs.

For more details, please find in BioRxiv doi: 10.1101/2021.11.24.469776.

Engineered ACE2-Fc potently snatch RBD and cross-neutralize SARS-CoV-2 VOCs.

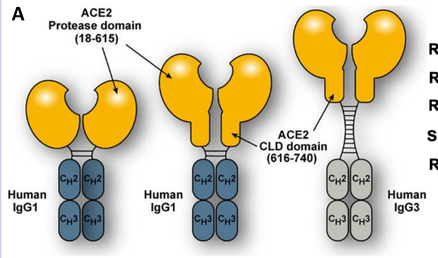

B

		ACE2 domain	*IgG backbone*
ACE2(18-615)	M14	monomeric ACE2-WT	-
	M27	WT	IgG1
	M33	H374A+H378A	IgG1
	M38	L79F+M82Y	IgG1
	M39	F28S+K31R	IgG1
	M40	L45D	IgG1
	M41	Q325Y	IgG1
	M86	L79F+M82Y+Q325Y+H374A+H378A LFMYQY2HA	IgG1 GASDALIE
ACE2(18-740)	M31	WT	IgG1
	M55	L79F+M82YQ325Y+H374A+H378A LFMYQY2HA	IgG1
	M58		IgG1 LALA
	M81		IgG1 GASDALIE
	M79		IgG3 (full hinge)
	M80		IgG3 (truncated hinge)

C **Heatmap of SPR K_D (nM)**

	M27	M33	M38	M39	M40	M41	M86	M31	M58	M79	M81
RBD_{SARS2}	26.0	27.6	4.67	63.6	19.7	9.14	3.58	13.9	3.35	4.98	2.74
$RBD_{B.1.1.7}$	24.8	23.6	8.02	89.8	34.6	11.8	4.78	18.1	3.72	16.0	2.89
$RBD_{B.1.351}$	11.6	7.70	3.82	75.5	28.4	7.95	1.59	8.38	1.33	4.77	0.87
Spike-6P	1.82	1.88	0.59	NA	1.76	2.14	0.53	1.02	0.89	0.69	0.76
RBD_{SARS1}	126	116	9.55	NA	NA	86.0	12.9	66.5	25.8	22.1	17.4

D **Pseudovirus neutralization IC_{50} (nM)**

	M14	M27	M31	M81	M86
SARS-CoV-2 S (WT)	>50	21.23	12.68	2.92	8.09
SARS-CoV-2 S (D614G)	>50	21.30	7.21	0.23	1.06
SARS-CoV-2 S (B.1.1.7)	17.97	6.62	4.80	0.52	1.15
SARS-CoV-2 S (B.1.351)	39.85	23.77	17.80	1.14	5.86
SARS-CoV-2 S (B.1.429)	>50	18.25	8.93	0.59	3.00
SARS-CoV-2 S (P.1)	31.45	12.76	6.63	0.24	2.17
SARS-CoV-2 S (B.1.526)	>50	>50	12.95	2.06	6.10
SARS-CoV-2 S (B.1.617.2)	24.86	10.54	3.99	0.76	2.28

A. Schematic of bivalent ACE2-Fc fusions.
B. A list of the developed ACE2-Fc variants.
C. Summary of SPR measurement of flow antigens to immobilized ACE2-Fc.
D. Heat-map summary of S-pseudotyped lentivirus neutralization IC_{50} for ACE2-Fc variants.

Structural basis for RBD binding enhancement and active-site rearrangement.

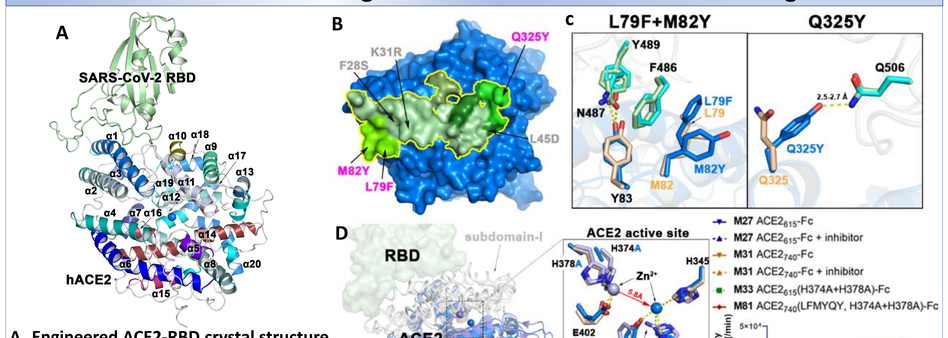

A. Engineered ACE2-RBD crystal structure.
B. RBD footprint on ACE2 surface.
C. L79F+M82Y optimize packing with RBD ridge and Q325Y adds an H-bond to RBD.
D. Zn^{2+}-disrupting mutations reshape the ACE2 active site and abolish enzyme activity.

ACE2(LFMYQY2HA) wtACE2 (6M0J) wtACE2-inhibitor (1R4L)

ACE2-Fc variants mediate robust Fc-effector functions *in vitro*.

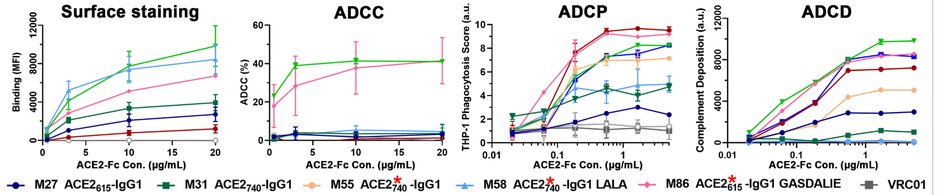

In-vivo efficacy of ACE-Fc depends on both neutralization and Fc-functions.

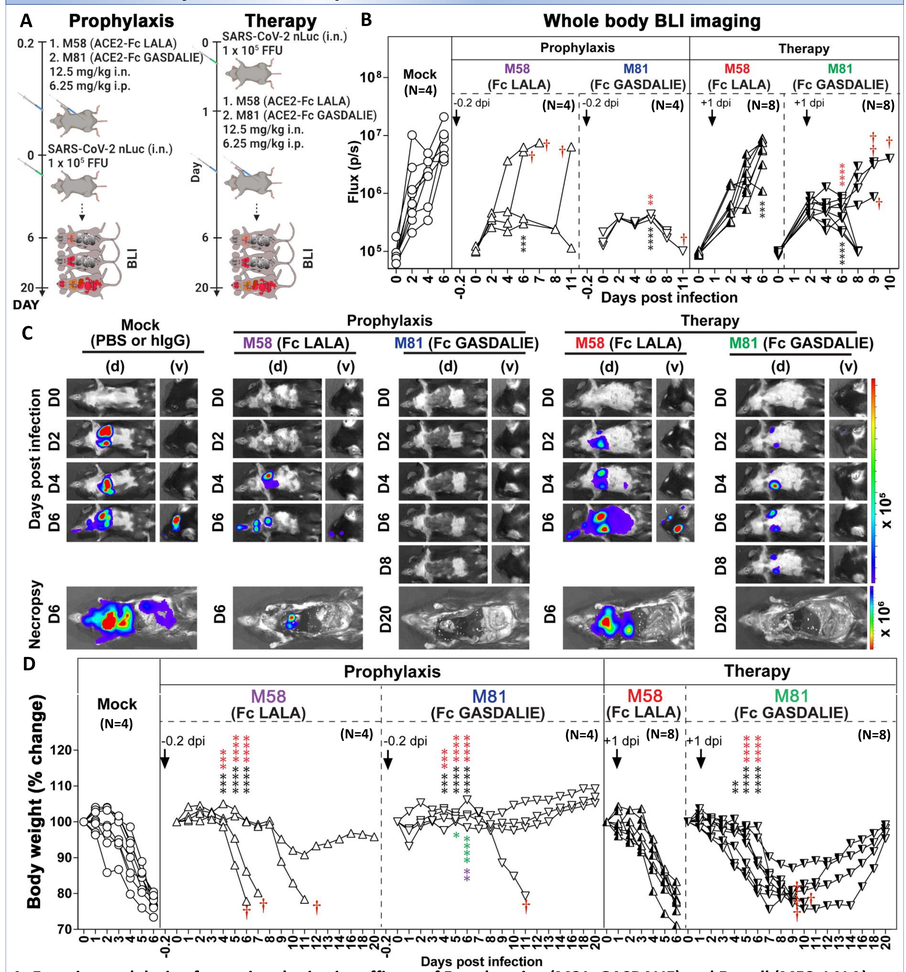

A. Experimental design for testing the *in vivo* efficacy of Fc-enhancing (M81, GASDALIE) and Fc-null (M58, LALA) ACE2-Fc. B. Temporal BLI quantification of the nLuc signal in the whole body. C. Representative BLI images of SARS-CoV-2 nLuc-infected mice in dorsal (d) and ventral (v). D. Temporal changes in mouse body weight compared to the initial body weight. Mice that succumbed to infection (cohorts not 100% mortality) are denoted with red daggers.

CONCLUSIONS

- **ACE2 mutations L79F+M82Y+Q325Y enhance SARS-CoV-2 RBD binding by ~13 folds. The lead variant, M81, neutralizes SARS-CoV-2 VOCs with sub-nanomolar IC_{50}.**
- **M81 with GASDALIE Fc mutations mediates potent Fc-effector functions *in-vitro* and *in-vivo*.**
- **Optimal ACE2-Fc therapeutic activity requires both neutralization and Fc-effector functions.**

Disclaimer: The views expressed in this presentation are those of the authors and do not reflect the official policy or position of the Uniformed Services University, the U.S. Army, the Department of Defense, the U.S. Government.

Conflicts of interest: The authors declare no conflict of interest.